A Metropolis Monte Carlo Method for Analyzing the Energetics and Dynamics of Lipopolysaccharide Supramolecular Structure and Organization

SEUNHO JUNG, DUGKI MIN, and RAWLE I. HOLLINGSWORTH*

Departments of Biochemistry, Computer Science, and Chemistry, Michigan State University, East Lansing, Michigan 48824

Received 16 August 1994; accepted 9 May 1995

ABSTRACT

A Metropolis Monte Carlo method has been developed for studying the effects of dielectric constant and counterion charge density and distribution on the energetics of formation and equilibria of the regular arrays or domain structures formed by bacterial lipopolysaccharides. The method utilizes a regular triangular prism primitive as a reductive structural representation of each lipopolysaccharide anchor (lipid A molecule). Charges for the two phosphate groups are localized at one apex and midway along the opposite side of the regular triangular top face of each prism. The counterions are not localized but are represented as a fine cloud of charge modeled by distributing the total charge over a fine two-dimensional cubic lattice. The six alkyl chains of the lipid A molecule are aligned along the long axes of the prism and are contained by its faces. All prisms are confined to the same plane but are allowed to translate within the plane and to rotate about axes perpendicular to the plane. The potential energy function contains an electrostatic term and a van der Waals term. A discontinuous dielectric is used to separate the aqueous and hydrophobic areas of the system. Trial moves involve both a rotational and a translational operation. The configurations predicted by this method are consistent with the crystal morphologies which have been observed for lipopolysaccharides. This analysis readily allows the evaluation of thermodynamic properties, such as heat capacity, entropy, and energy. The root mean square average separation of units was also calculated as a function of iteration number.

*Author to whom all correspondence should be addressed.

Journal of Computational Chemistry, Vol. 17, No. 2, 238–249 (1996)

CCC 0192-8651 / 96 / 020238-12

Introduction

Bacterial lipopolysaccharides are complex lipid-linked polysaccharides which reside in the outer membranes of gram-negative bacteria. The relatively invariant component of these molecules is the lipid anchor called the lipid A. In most bacteria, the lipid A is a glucosamine disaccharide containing six fatty acyl chains and two phosphate groups. It is the lipid A region which embodies the physical and biological properties of general interest in lipopolysaccharides. One characteristic property of lipopolysaccharide or lipid A molecules is their propensity to form regular supramolecular arrays with hexagonal symmetry.[1,2] Their ability to self-assemble into defined high-symmetry structures has potential for the development of intelligent materials and substrates for the design of advanced optical and electrical devices. The propensity to self-assemble into regular arrays may also be at the heart of the profound biological activities which these molecules exert when they interact with the mammalian immune system. This interaction leads to a cascade of cellular responses leading eventually to shock and death.[3] It is possible that this cascade of events may be triggered by a perturbation of some dynamic property(ies) of the host membrane. Numerous studies using a variety of techniques, including fluorescence depolarization and electron spin resonance, have shown lipopolysaccharide-induced dynamic changes in membrane systems.[4-6] Other studies have also indicated that the biological activities of lipopolysaccharide molecules depend on their counterion form.[7] We have demonstrated that biological activities of lipopolysaccharides can be offset by molecules which disrupt their supramolecular structure and/or increase the fluidity of the host cell.[8] To correlate the biological and physical properties of lipopolysaccharides and lipid A molecules with their chemical and supramolecular structure and with various environmental conditions, such as temperatures, pH, counterion type, and concentration and dielectric constant, is a formidable task. To do this, it is necessary to develop computational models and methods for predicting the supramolecular structure organization, equilibria, and energetics. Molecular dynamics methods are not easily applicable because of the size of the systems and the prohibitively long time scale over which the potential energy function must be integrated. Atomistic models are also impractical because of the very large number of pairwise nearest neighbor relationships. It therefore becomes necessary to develop a nonatomistic computational approach which will embody the key structural elements of the lipid A system. Such an approach would allow analysis of the order and phase behavior and the thermodynamics of formation of these complex systems. In this article we describe such a nonatomistic Metropolis Monte Carlo approach.

Methods

GENERAL METHODS

All computer code was written in the C language and complied on a SPARK Station 10 from SUN Microsystems Inc. using a C Development Set (CDS) SPARK Complier (version 2.0.1). Calculations were performed in a UNIX environment running SUN operating system, Solaris 2.3. The dimensions for the geometric primitives (triangles, circles, etc.) used to represent the lipid A structure were based on geometries calculated by the DREIDING[9] or MM2[10] molecular mechanics force fields, as implemented in the program BIOGRAF,[11] or were abstracted from those parameter sets. The molecular mechanics programs were implemented on a Silicon Graphics IRIS 4D-310 or 4D-70 GTX computer using the IRIX operating system (version 4.0.1).

THE SYMBOLIC REPRESENTATION OF LIPID A STRUCTURE

The model on which the calculations are based is a geometric reduction of the three-dimensional model proposed for the minimum-energy conformation of the lipid A molecule[12] (Figs. 1a–c). This structure was proposed based on a combination of information from molecular mechanics calculation, infrared (IR) and nuclear magnetic resonance (NMR) measurements, and X-ray power diffraction studies. In the geometric reduction, the six alkyl chains of the lipid A molecule are represented as six parallel, packed cylinders. The top view of this arrangement is then six circles arranged to form an equilateral triangle. The circles are all in the same plane. The primary parameters which are derived from this representation are the coordinates of the center of the cross section of

(a)

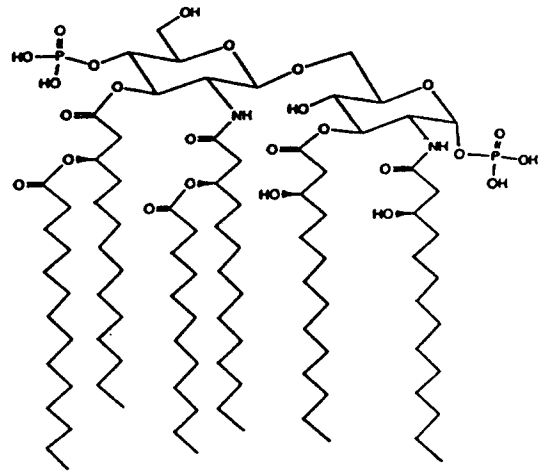

FIGURE 1. (a) Structure of the lipid A of *E. coli* lipopolysaccharide. (b) Side view of a model of the E. coli lipid A molecule as determined by a combination of physical and computational methods. (c) Top view.

(b)

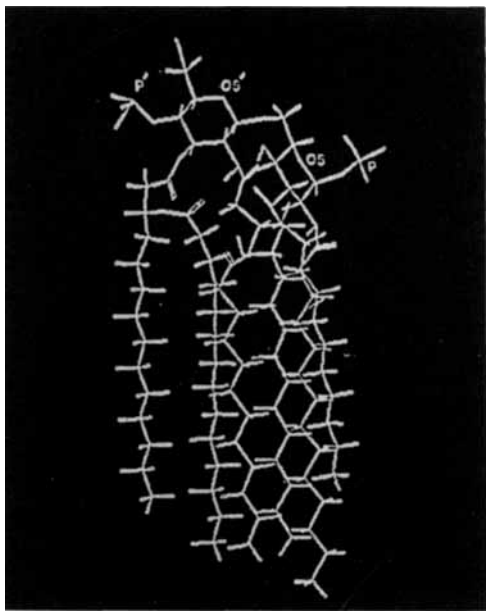

FIGURE 1. (*Continued*).

each lipid chain or the coordinates of the center of each circle. These coordinates are obtained from the dimensions of a triangle which can be circumscribed by a circle, which just touches the outermost three of the six circles representing the lipid chains (Fig. 2). The center of this inscribed triangle (or the center of the circumscribed circle) is a primary reference coordinate and is assigned the coordinate labels (a_0, b_0). Three other reference coordinates are the points where the circumscribed

(c)

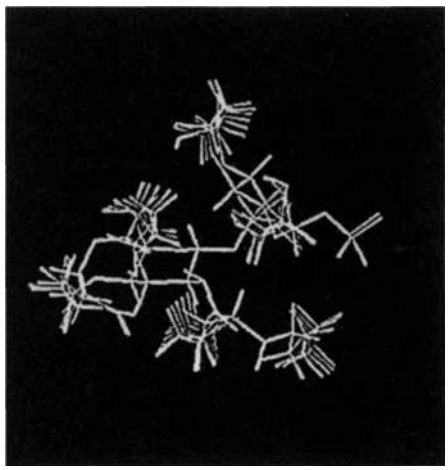

FIGURE 1. (*Continued*).

circle touches the inscribed triangle. The coordinates of the center of the cross section of each lipid chain (f_i) are determined primarily, relative to the coordinate (a_0, b_0) and the three other reference coordinates. Charges for the phosphate groups are localized at one apex and midway along the opposite side of the top triangular face of each prism, as indicated in Figure 2.

POSITION AND ORIENTATION OF MOLECULES IN CONFIGURATIONAL SPACE

The positions of the geometrically reduced lipid A structures were mapped in two-dimensional configuration space by assigning the centers of their circumscribed circles to points on a two-dimensional hexagonal grid. The hexagonal geometry was chosen to allow maximum interaction (closest packing) between the molecules. Alternating rows and columns of a hexagonal lattice form a cubic lattice and, provided that the lattice is fine enough, remove any configurational bias which the choice of lattice might have on the outcome of the simulation. At the beginning of the simulation, the center of each symbolic triangle (or its circumscribed circle) was randomly assigned to a lattice point in a rectangular coordinate system. The coordinates of any such lattice point were designated by C_{ij}. The dimensionality of the available coordinate space for placement (position) of the lipid A primitives was, therefore, Σ_{ij}, a variable depending on the size of the simulation and the computational resources which are available. The dimensionality of the space was chosen to be significantly greater than the number of primitives

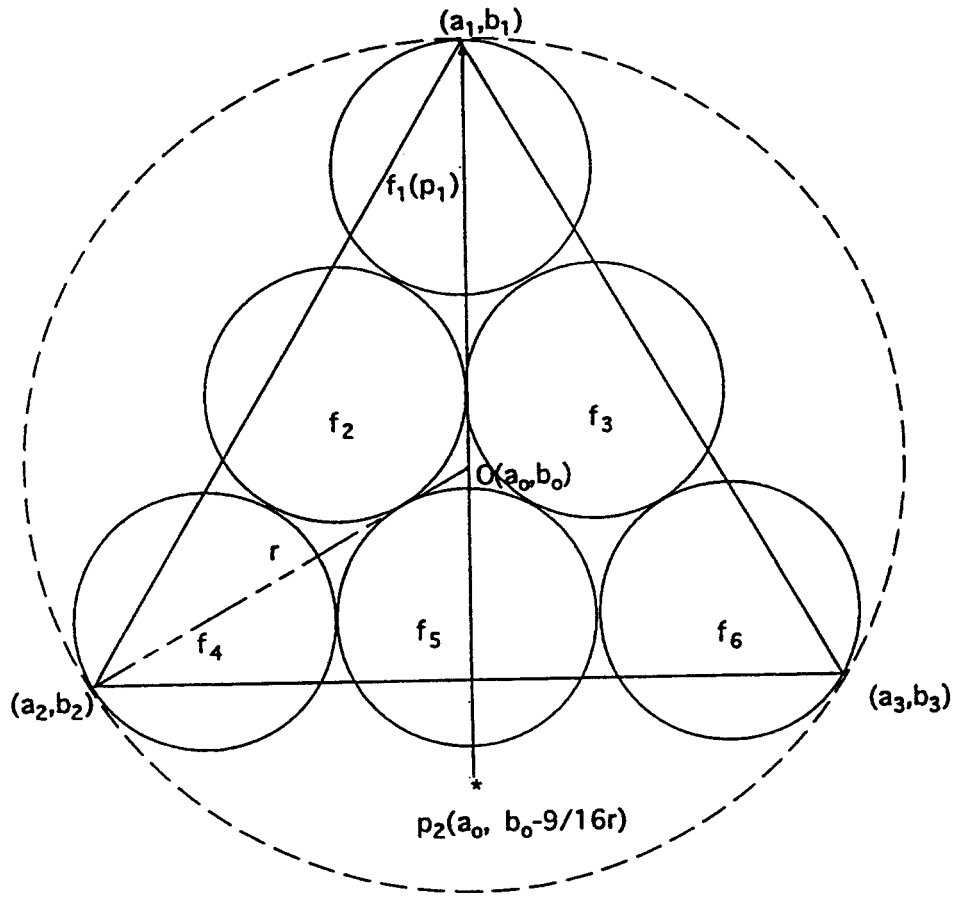

FIGURE 2. Top view of a lipid A primitive. Each solid circle represents a fatty acyl chain in the lipid A molecule; r is the radius of the circumscribed circle, f_i indicates the coordinates of the center of the cross section of the ith alkyl chain, p_1 and p_2 indicate the two phosphate groups. Phosphate 1 (p_1) is located at the center of circle f_1. Each value of f_i was calculated in terms of the coordinate of the origin ($O(a_0, b_0)$ and the three apexes of the circumscribed circle.
$f_1 = (4/13*(4 - \sqrt{3}(a_1 - a_0) + a_0,\ 4/13*(4 - \sqrt{3}(b_1 - b_0) + b_0)$; $f_2 = (4/13*(4 - \sqrt{3}(a_1 + a_2)/2 - a_0) + a_0$,
$4/13*(4 - \sqrt{3}(b_1 + b_2) - b_0) + b_0)$; $f_3 = (4/13*(4 - \sqrt{3}(a_1 + a_3)/2 - a_0) + a_0$,
$4/13*(4 - \sqrt{3}(b_1 + b_3) - b_0) + b_0)$; $f_4 = (4/13*(4 - \sqrt{3}(a_2 - a_0) + a_0$,
$4/13*(4 - \sqrt{3}(b_2 - b_0) + b_0)$; $f_5 = (4/13*(4 - \sqrt{3}(a_2 + a_3)/2 - a_0) + a_0$,
$4/13*(4 - \sqrt{3}(b_2 + b_3) - b_0) + b_0)$; $f_6 = (4/13*(4 - \sqrt{3}(a_3 - a_0) + a_0,\ 4/13*(4 - \sqrt{3}(b_3 + b_0) + b_0)$.

used in the simulation so that the starting configuration would not influence the outcome of the calculations. The lattice points were separated by α Å in the horizontal direction, and the rows were separated by $(\alpha\sqrt{3})/2$ Å in the vertical direction (Fig. 3). The distance between any two neighboring lattice points in any direction was therefore α. The magnitude of the lattice point separation (α) was chosen to be less than $2r$, where r is the radius of the circumscribed circle of the lipid A primitive. These circles, therefore, overlapped if they were assigned to adjacent lattice points. The value of α was chosen to ensure good van der Waals contact between the molecules but reduce the frequency of bad contacts. Even though the circumscribed circles overlap, the triangular primitives do not necessarily do so. The value of α can be varied from simulation to simulation. The value of R (from molecular mechanics calculations) is 4.10 Å, and the default value of α used was 6.00 Å. The position $C(i, j)$ of any grid point could be calculated from the following expression:

$$C(i,j) = (a_0 + \varepsilon_a*(j-1),\ b_0 + \varepsilon_b*(i-1);$$
$$i = 1,3,5,\ldots,2k-1,\ldots,\quad j = 1,2,3,\ldots \quad (1)$$
$$C(i,j) = (a_0 + \varepsilon_1*(j-1.5),\ b_0 + \varepsilon*(i-1);$$
$$i = 2,4,6,\ldots,2k,\ldots,\quad j = 1,2,3,\ldots \quad (2)$$
$$\varepsilon_a = 2\sqrt{3} - 2,\quad \varepsilon_b = 3 - \sqrt{3} \quad (3)$$

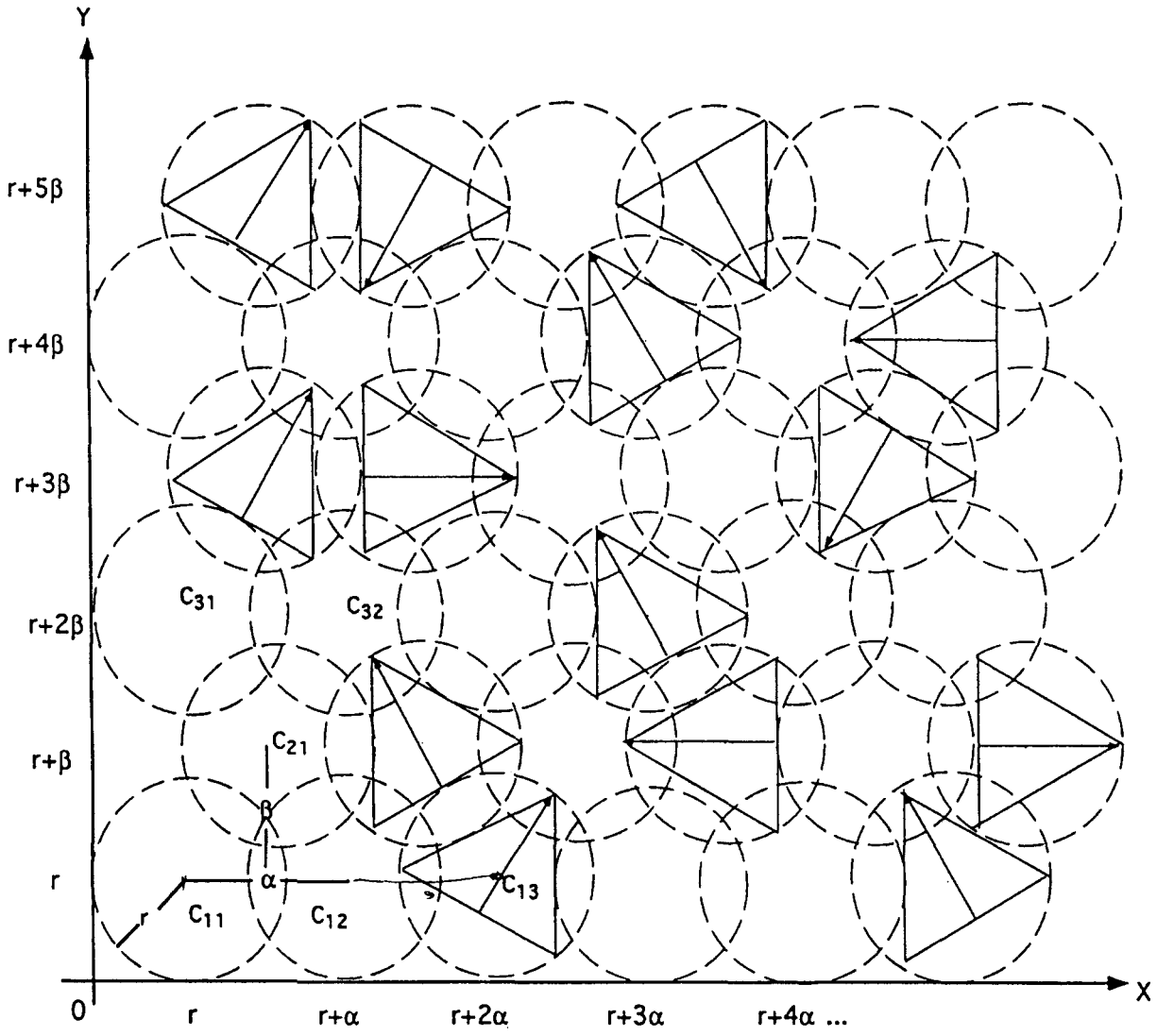

FIGURE 3. Generalized hexagonal coordinate system $[C(i, j)]$ in the X- and Y-planes. $C(i, j)$ indicates the coordinates of the center of the circumscribed circle of a lipid A primitive and r indicates its radius, α is the separation distance along the X-axis, and β is the separation along the Y-axis. Since $C(1, 1)$ is (r, r), all other coordinates $[C(i, j)]$ can be represented as a function of r and α. $C(i, j) = (r + (j - 1)\alpha, r + (i - 1)\beta)$, $i = 1, 3, 5 \ldots 2k - 1 \ldots$ $C(i, j) = (r + (j - 1/2)\alpha, r + (i - 1)\beta)$, $i = 2, 4, 6 \ldots 2k$. In this figure, $\beta = a\sqrt{3}/2$. The arrow indicates the relative positions of the two phosphate group ($1 \Rightarrow 4$ direction).

The matrix size for the simulation was controlled by changing the values of Σ_{ij}. In this coordinate system, the coordinates of the first lattice point are (r, r). One such local rectangular coordinate system was used to represent each cell in simulations involving periodic boundary conditions.

In calculations using periodic boundary conditions, the local rectangular coordinate system $C(i, j)$ which describes the positions of the lipid A primitives in configurational space (Fig. 3) for each cell could be easily translated into a Cartesian coordinate system in which each point in the lattice of each image cell was then referenced relative to a common origin. This ensured that each element in the entire system could be tracked in a global fashion.

Once the position of each lipid A primitive could be mapped, the next step was to define their orientations. These were also assigned random attributes, but trial moves were restricted to any of six randomly assigned orientations separated from each other by 60° (Fig. 4). The algorithm allows for

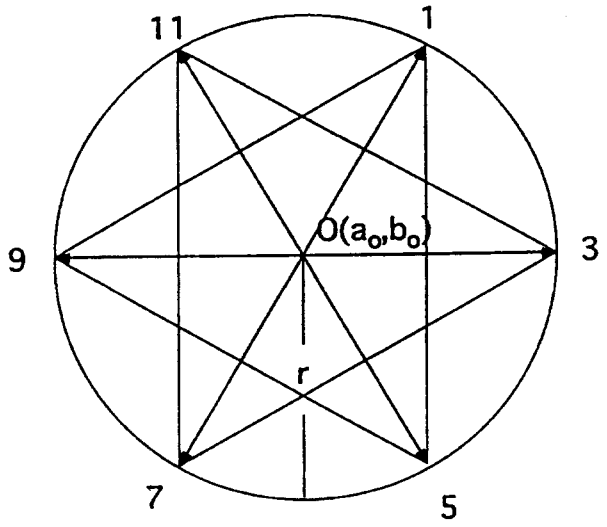

FIGURE 4. Orientation of a lipid A primitive in rotational phase space. Depending on the position of two phosphate groups (indicated by an arrow), the rotational orientation can be defined. The orientation can be encoded by the numbers (1 –11) at the apexes. $O(a_0, b_0)$ indicates the coordinate of the center of a primitive, and r indicates the radius of the circumscribed coordinate circle of a lipid A primitive. The encoded coordinates (1 –11) of each apex are written in terms of radius (r) and the coordinate ($O(a_0, b_0)$): $1 = (a_0 + r/2, b_0 + \sqrt{3}/2)$, $3 = (a_0 + r, b_0)$, $5 = (a_0 + r/2, b_0 - \sqrt{3}/2)$, $7 = (a_0 - r/2, b_0 - \sqrt{3}/2)$, $9 = (a_0 - r, b_0)$; $11 = (a_0 - r/2, b_0 + \sqrt{3}/2)$.

much smaller division of this rotational orientation space, but the actual value chosen was largely determined by computational resources. Hence, for six lipid A molecules (triangular primitives) there would be 46,656 total possible rotational configurations. It is important to note that although none of these are redundant with respect to the orientation of charged groups, many of them are with respect to the orientation of the alkyl chains since the primitives (without the charged groups) have three-fold symmetry. Changing the size of the step to 30° increments and using the same number of primitives increases the total number of possible orientations (including degeneracies) to over 2 billion.

The electrostatic charge contribution was modeled by evaluating the electrostatic potential between the charged groups of the lipid A molecule and a continuous grid of positive charge which represented the counterion charge cloud. A rectangular, finely-divided two-dimensional grid in which each cell has equal dimensions and sides of equal lengths was constructed above the plane of the lipid A molecules at a distance which could be varied (Fig. 5). The total counterion charge divided by the total number of grid points) was located at each point. The default size of the charge array was 44 × 44 grid points. By increasing the total pixel density of the grid, the counterion charge cloud could be made to approach as a continuum. A discontinuous dielectric model was used to treat the dielectric constant of the medium surrounding the molecules. This was accomplished by dividing the total volume containing the molecules into two regions of different dielectric constant by placing a boundary at the interface between the regions representing the hydrophobic lipid chain and the aqueous milieu of the lipid A head group containing the phosphate substituents. The upper region containing the counterion charge cloud and phosphate groups was assigned one of 78.7, the dielectric constant of water. This value could be varied as an input variable. The effective counterion charge in the region of the plane containing the phosphate groups could be varied by altering the separation between that plane and the one containing the cation cloud.

THE FORCE FIELD

Two terms were used in the force field for calculating the potential energy of the system. These were an electrostatic term and a van der

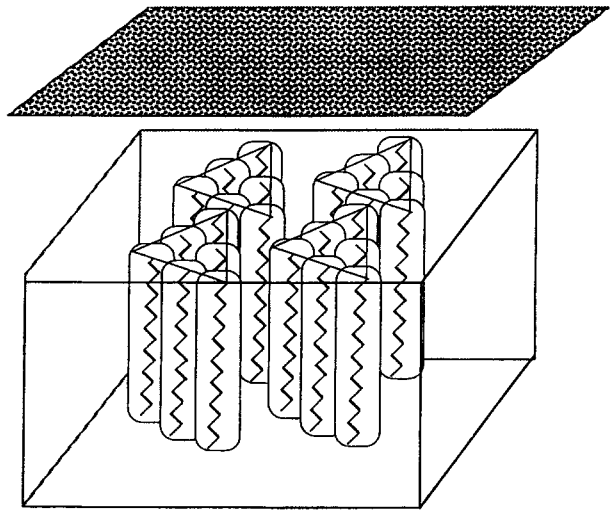

FIGURE 5. View of a charge cloud and the lipid A primitives. The density of pixels and the relative distance between the charge plane and the plane containing the surfaces of the primitives could be defined in each simulation.

Waals term. The electrostatic term was evaluated according to the expression

$$E_e = -q_1 q_2 / Ad \quad (4)$$

Here, E_e is the electrostatic energyl, q_1 and q_2 are the charges at sites 1 and 2, A is a constant (332.0637 Coulombs^2 kcal^{-1} Å^{-1}), and d is the separation between sites 1 and 2. Electrostatic terms are summed over interactions involving pairs of phosphate groups and between each phosphate group and fractional charges on the counterion grid within a given cutoff radius, the default value of which was 12 Å. This is another input parameter that can be increased or decreased depending on the computational resources available. Most commercial molecular mechanics packages have a default distance of 10 Å.

The van der Waals interactions were calculated according to a method introduced by Salem.[13] Instead of evaluating explicitly each pairwise interaction potential between methylene groups, the van der Waals interactions between the extended hydrocarbon chains were determined using eq. (5):

$$E_{\mathrm{vdW}} = B(3\pi n / 8 l^2 D^5) \quad (5)$$

Here l is the length of the hydrocarbon chain per methylene group, n is the number of methylene groups in a chain, D is the separation between two alkyl chains, L is the length of the alkyl chains, and B is a constant (-1340 Å kcal/mol). This term was evaluated for all alkyl chains within a cutoff distance of 12 Å of each other. The equation is valid for instances in which the length of the chains is large compared to their separation ($L \gg D$).

MONTE CARLO SIMULATION

The general strategy for carrying out the Monte Carlo method simulation is as follows. The first step was to set up and define the original (random) positions and orientations of the lipid A primitives. This also involved defining cutoff distances, charges, the separation between the counterion grid and the plane containing the lipid A primitives, the pixel density of the counterion grid, the dimensionality Σ_{ij}, the number of cells in the periodic array, dielectric constants, the number of primitives used in the simulation, the separation (α), the density of the lattice points (i, j), and the charges on the phosphate groups. The next step in the simulation was to generate a new set of random coordinates for the lipid A primitives. This was accomplished by adding a random increment or offset to each positional or rotational coordinate of each primitive. The energy of the new configuration was then evaluated and the new configuration was accepted or rejected according to the Metropolis criteria.[14] If the energy of the new configuration was equal to or less than that of the previous configuration, it was accepted. However, if it was greater, a random number between 0 and 1 was generated and the quantity $e^{-\Delta E/kT}$ was evaluated. If this latter quantity was greater than or equal to the random number, the new configuration was accepted; if it was less, it was rejected. The primary data collected were the separate electrostatic and van der Waals interaction energies as a function of the configuration number.

Results

The total energy of the system was evaluated using various values for the dimensionality (determined by Σ_{ij}) of the two-dimensional grid over which the triangular primitives were allowed to move. This effectively varied the spatial constraints, thus allowing convergence to equilibrium configurational distributions which reflected the packing density. The Monte Carlo average energy ($\langle E \rangle$) was evaluated using the relation

$$\langle E \rangle = (1/M) \Sigma E_i \quad (6)$$

where M is the number of steps leading to the ith iteration and E_i is its energy.

The different packing densities (unit cell dimension) also has a profound influence on the approach to equilibrium on the Monte Carlo time scale. Hence the configuration number at which the energy converged occurred progressively later as the dimension of the unit cell was increased (Fig. 6). In addition, the energy started to become independent of dimensionalities greater than 81, indicating that finite size limitations are no longer influencing the result. An analysis of the configurations of the interacting triangular primitives indicated that there was a distribution of interacting states (aggregates) with various levels of association (Fig. 7a). In the simulations in which the dimensionality was 16, several hexagonal clusters (hexamers) could be observed once the energy distribution converged (Fig. 7b). The interacting states were observed to be distributed between dimers, trimers, tetramers, pentamers, and hexa-

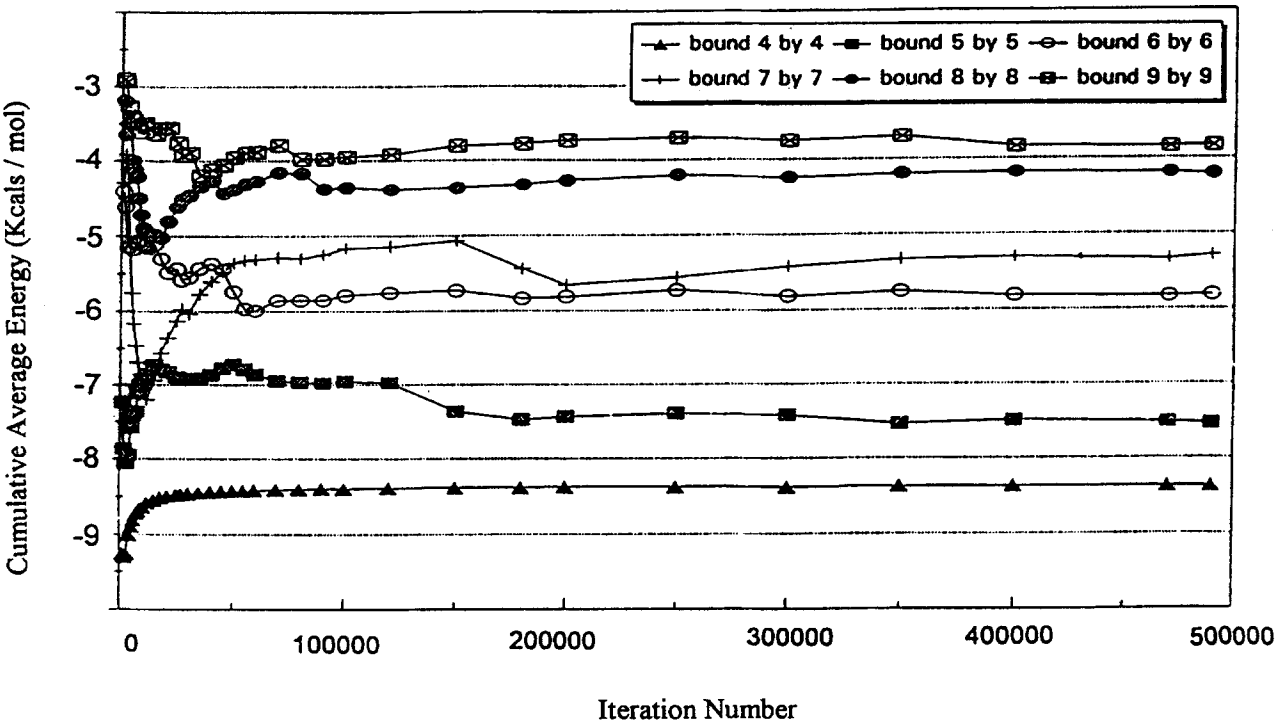

FIGURE 6. The cumulative Monte Carlo average energy as a function of dimensionality for six lipid A molecules per unit cell in a 3 × 3 periodic array (54 lipid A molecules total). The dimensionality of each unit cell was varied from 16 (4 × 4) to 81 (9 × 9).

mers. There was also a monomer population. The energies of these different aggregate forms (microstates) were found to be separated into nonoverlapping levels or bands, thus allowing effective coarse-graining and the enumeration of the probability or frequency of occurrence of the different microstates (Fig. 8a). Microstates were defined as configurations in which the triangular primitives have the same total number of interacting edges. Hence a configuration in which the six primitives in a unit cell were arranged as two edge-to-edge dimers and two monomers had a similar energy to one in which there was one trimer (again two shared edges) and three monomers. The energies of each level (population of microstates), however, could be further decomposed into microstates based on symmetry considerations. The calculations were also carried out without the electrostatic term in the force field. This also led to the same coarse-graining of microstates, except that the hexamer configuration was now much more common (Fig. 8b). The probability of occurrence of the microstates of higher order (hexamers and pentamers) was considerably higher when the freedom of the system was more constrained. The frequency (probability) distribution could be fitted to a smooth curve with a cubic spline function, and its general form reflected the Boltzmann statistics underlying the Metropolis algorithm (Fig. 9). The mean energy was observed to shift toward higher (attractive) interaction energy, and the frequency (probability) distribution curve was significantly narrower as the dimensionality of each unit cell decreased. Again, relaxation of finite size effects was observed since the system reached a limiting value of ~32% for the probability of the most common configuration (between two and three interacting edges).9

Discussion

The order, dynamics, and energetics of the phase transitions of two-dimensional systems are an area of intense interest in the physics and chemistry of condensed matter systems.[15] In this context, the calculation of the bond order and related macroscopic properties of two-dimensional systems has

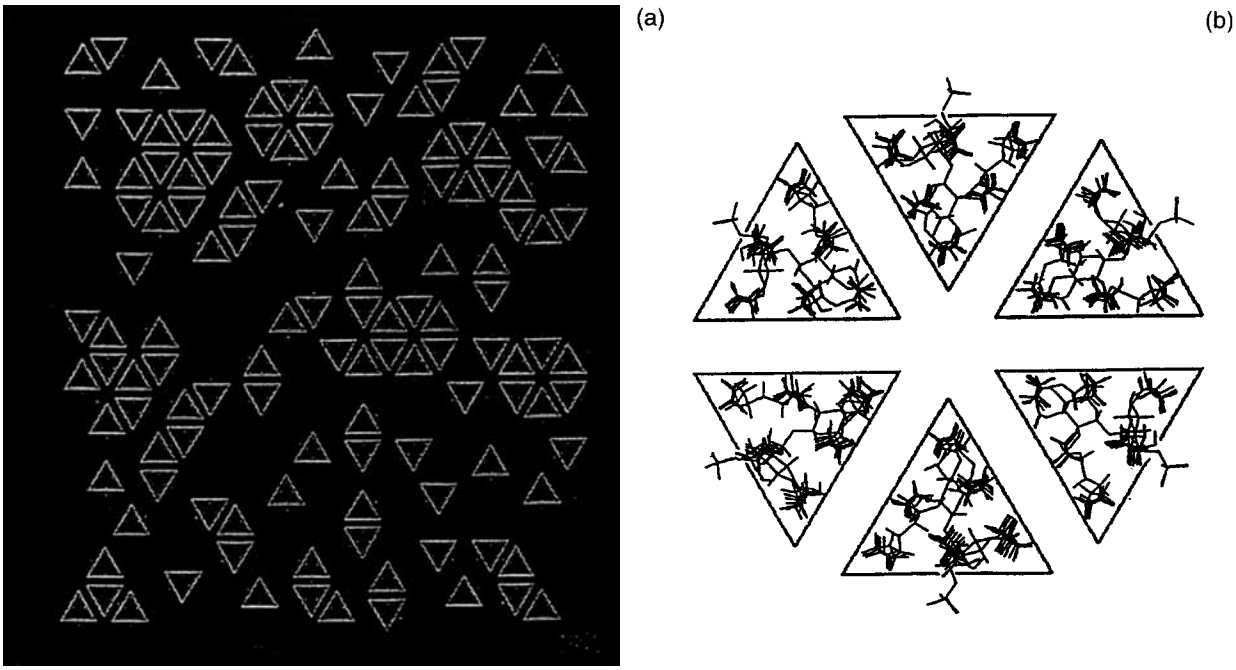

FIGURE 7. (a) Result of simulation involving 128 lipid A primitives per unit cell with a dimensionality of 400 (20 × 20) performed under periodic boundary conditions. Note the formation of regular hexagonal systems. (b) The configuration of one of the hexagonal systems.

received much attention.[16] This has proven to be important both for explaining and predicting their observed short-range and long-range order and their thermodynamic properties. It is often impossible given the current computational resources, to develop atomistic models for carrying out these calculations. Symbolic models, in which geometric shapes embody the desirable spatial and physical attributes of the molecular system, are often devised. Hence the Penrose tiling and other models are often used for studying the two-dimensional (hexatic) ordering of molecular systems.[16] The approach used here to study lipid A order is similar in philosophy to these since the essential elements of lipid A size, geometry, and charge are represented in a highly symmetrical structural surrogate. The hexagonal structure of the cluster of triangular prisms shown in Figure 7b is consistent with the macroscopy structure observed for lipid A crystals and films by electron microscopy.[1,2] In one of the studies,[2] lipopolysaccharides were observed to form perfect hexagonal plates. In both studies, a periodic, hexagonal array of lipids was observed if the lipid A or lipopolysaccharide was allowed to form a layer on the grid by drying an aqueous solution. Although the force field used here is a simple one, it is rigorously rooted in theory and should still realistically and quantitatively represent the important dispersive and electrostatic components of the intermolecular interactions. The results of the computations performed here readily lead themselves to a rigorous statistical analysis since the energies of the microstates fall into defined levels. One can, therefore, evaluate entropies and partition functions directly and explore the relative importance of disorder (high entropy) and order (stable energy) in determining the supramolecular structure of these molecules. The root mean square average separation between units, the specific heat (C_v), the cumulative average Monte Carlo energy, and the entropy of a system containing a total of 54 lipid A molecules were determined (Figs. 10a–d) with and without an electrostatic term in the potential energy function. These calculations can be performed routinely by the program with any number of primitives, dimensionality, and image cells (the computational resources are the only limitation). They are standard input/output functions. It is readily observable that the behaviour and properties of these systems are dominated by the van der Waals term. This is true largely because of the high symmetry of the lipid A molecule and the high packing efficiency (and extent of alkyl chain

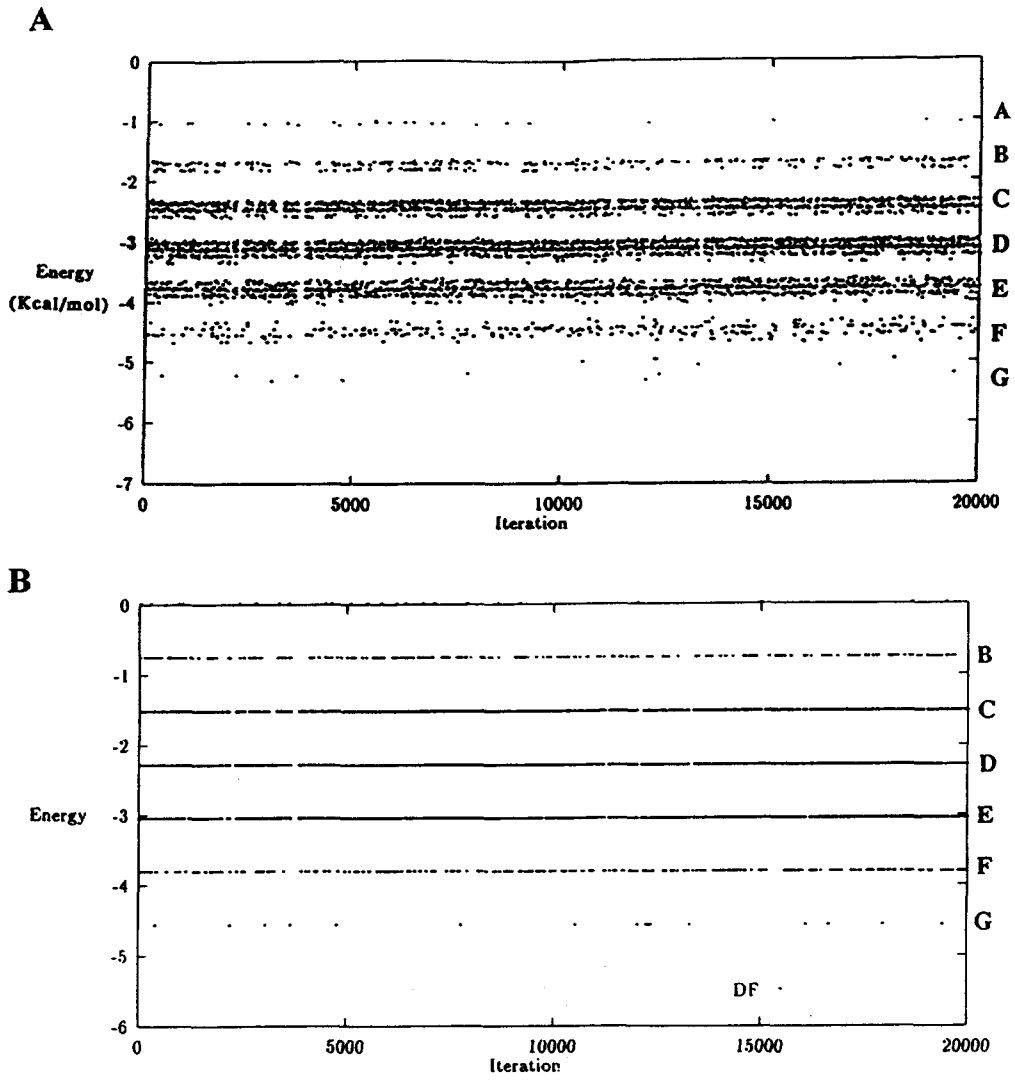

FIGURE 8. (a) Energies of configurations as a function of Monte Carlo step. Note the coarse-graining of the different microstates. The level labeled A corresponds to microstates, in which the units are completely separated and non-interacting. Level B corresponds to microstates containing only one dimer (one common face between units). Level C corresponds to microstates containing two dimers or one trimer with no other interactions (two common faces). Levels D, E, F, and G correspond to microstates containing three, four, five, and six common faces, respectively. Six common faces correspond to hexagonal order (Fig. 7b). (b) Similar calculation in which the electrostatic term is left out of the potential energy function (van der Waals interaction only).

contact) that results from it.

One obvious feature of the calculations performed on smaller systems was the effect of finite size restrictions on the final outcome. Hence, in the calculation of the cumulative energy using varying dimensionalities (Fig. 6) and the distribution of microstates as a function of dimensionality (Fig. 9), these effects were easily discernible. Despite this, it was also clear that there was convergence toward a limiting value of energy (in the first case) and the most probable microstate (in the second) as the dimensionality of the system was increased. Enumeration of microstates is usually only possible in small systems, and the exercise on such scales is usually only of academic interest. The extent of coarse-graining observed here, and even in much larger systems, makes calculation of an entropy parameter possible.

One of the primary reasons for developing this computational method was to allow calculation of the lowest-energy configurations of lipid A units in an ensemble and to evaluate the relative contri-

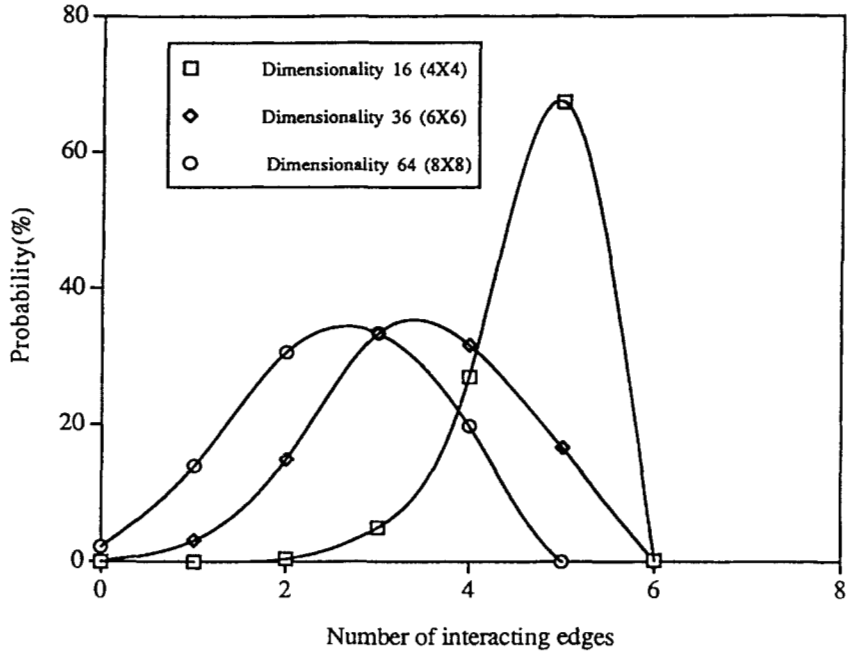

FIGURE 9. Frequency of occurence of different microstates as a function of the dimensionality of the unit cell.

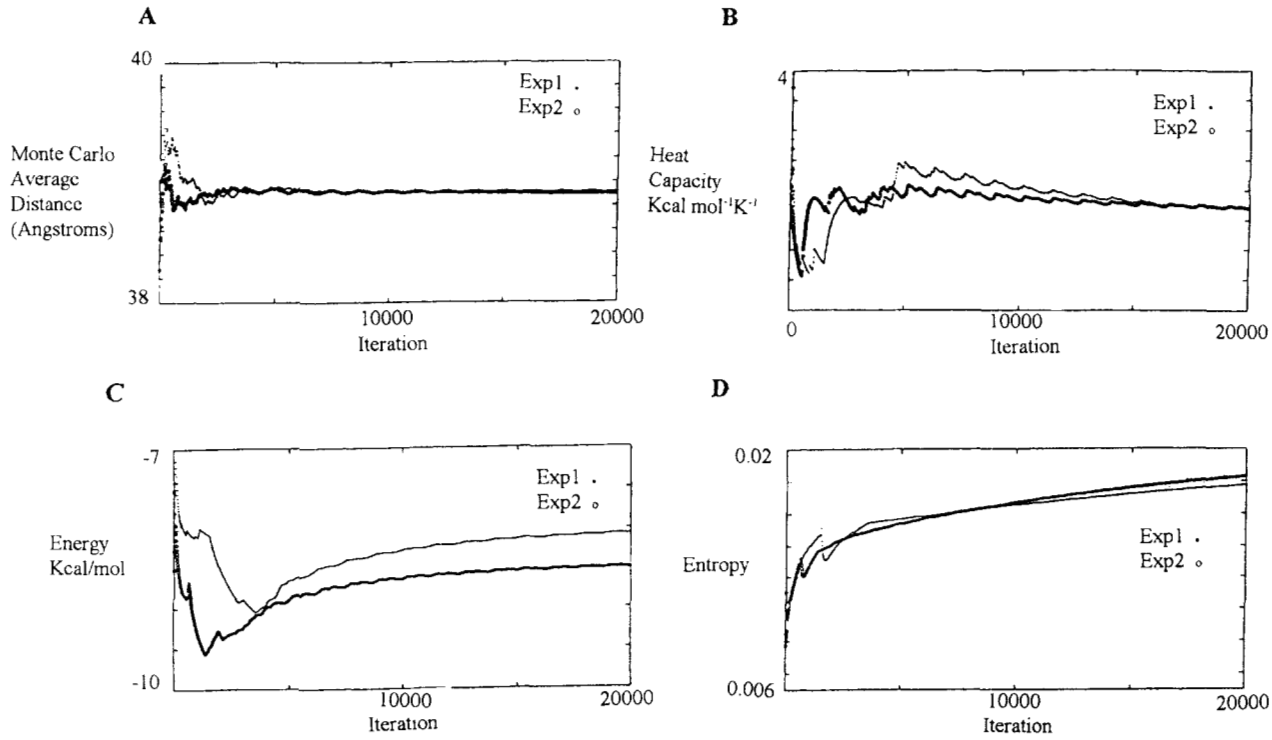

FIGURE 10. Results from the calculation of (a) root mean square average separation of units, (b) head capacity, (c) Monte Carlo energy, and (d) entropy as a function of iteration number. Calculations were performed for a system containing a total of 54 lipid A primitives under periodic boundary conditions. Small circles denote calculations done using a van der Waals term only (EXPT 1), and large circles denote calculations done using the full potential energy function (EXPT 2). Heat capacity (C_v) was evaluated using the standard expression $C_v = (\sigma_E)^2 / kT$, where $(\sigma_E)^2$ is the energy fluctuation and k is the Boltzmann constant. Entropy was calculated using the usual relationship $S = -\Sigma p_i \ln p_i$, where p_i is the probability of energy state E_i occurring. The summation is carried out over the total number of possible states.

butions of electrostatic and van der Waals interactions in the overall stabilization. The nonatomistic approach used here will allow the treatment of large arrays, in which case finite size effects should not even be discernible. The effects of charge density of the counterions in the lipid head groups can readily be evaluated. So can the effects of pH (leading to changes in the formal charge of the phosphate group), temperature (which modifies the dielectric constant, changes the Boltzmann factor, and increases the mean separation of lipid units), static electric fields, and changes in the dielectric constant of the head group region. The effect of loss of either phosphate group from the lipid A molecule or their replacement by other charged groups and the effect(s) of molecules that partition into the hydrophobic bulk of the alkyl chains and disrupt the packing (thus reducing the van der Waals contribution) on the stability of the lipid A system can also be assessed.

Acknowledgments

This work was supported by grant DE-FG02-89ER14029 from the U.S. Department of Energy to R. I. H and by the Michigan State University Center for Microbial Ecology, a National Science Foundation Science and Technology Center (BIR 912-0006).

References

1. J. W. Shands and K. Nath, *J. Molec. Biol.*, **25**, 15 (1967).
2. N. Kato, *Micron*, **24**, 91 (1993).
3. A. Nowotny, *Bacteriol. Rev.*, **33**, 72 (1969).
4. R. Price and D. Jacobs, *Biochim. Biophys. Acta*, **859**, 26 (1986).
5. N. Larsen, R. Enelow, E. Simons, and R. Sullivan, *Biochim. Biophys. Acta*, **815**, 1 (1985).
6. S. K. Jackson, P. E. James, C. C. Rowlands, and I. C. Evans, *Free Rad. Res. Commun.*, **8**, 47 53 (1989).
7. C. Galanos and O. Luderitz, In *Handbook of Endotoxin*, Vol. 1, E. Th. Rietschel, Ed., Elsevier, Amsterdam, 1984, p. 46.
8. K. Kim, D. Lill-Elghanian, and R. I. Hollingsworth, *Bioorg. and Med. Chem. Lett.*, 4, 1691 (1994).
9. S. L. Mayo, B. D. Olafson, and W. A. Goddard III, *J. Phys. Chem.*, **94**, 8897 (1990).
10. T. Liljefors, J. C. Tai, S. Li, and N. Allinger, *J. Comp. Chem.*, **8**, 1051 (1987).
11. Molecular Simulations, Inc., Waltham, MA 02154.
12. R. Hollingsworth, S. Jung, K. Kim, and D. Lill-Elghanian, *International Symposium on Nucleic Acids and Membranes*, Vancouver, British Columbia, May 1993.
13. L. Salem, *Can. J. Biochem. Physiol.*, **40**, 1287 (1962).
14. N. Metropolis, A. W. Rosenbluth, M. N. Rosenbluth, and A. H. Teller, *J. Chem. Phys.*, **21**, 1087 (1953).
15. J. D. Brock, In *Bond Orientational Order in Condensed Matter Systems*, K. Strandburg, Ed., Springer-Verlag, New York, 1992, p. 1–31.
16. K. Strandburg, In *Bond Orientational Order in Condensed Matter Systems*, K. Strandburg, Ed., Springer-Verlag, New York, 1992, p. 210–237.